The MEG experiment at Lecce

G. Chiarello,[1 2] C. Chiri,[2] G. Cocciolo,[1 2] A. Corvaglia,[2] A. Innocente,[2] F. Grancagnolo,[2] A. Miccoli,[2] M. Panareo,[1 2] A. Pepino,[1 2] C. Pinto,[1 2] G. Rispoli,[1 2] M. Spedicato,[1] G.F. Tassielli[1 2]

[1]Dipartimento di Fisica, Università del Salento, Italy

[2]Istituto Nazionale di Fisica Nucleare sez. di Lecce, Italy

1. Introduction

The Lepton Flavour Violation in the charged lepton sector (cLFV) is forbidden in the Standard Model (SM). Even in the extensions of SM with neutrino masses and oscillation, cLFV is expected at the level of BR($\mu^+ \rightarrow e^+\gamma$)<$10^{-54}$, which cannot be experimentally observed with any current experimental approach.

Conversely, New Physics (NP) models, developed to overcome the limitations of the SM, predict observable cLFV effects in a very natural way. In fact, cLFV is predicted by almost any NP model (Super-Symmetry (SUSY) and Grand Unification (GUT)) and the present experimental limits already strongly constrain the search for such theories [1].

One of the golden channels to search for new physics through cLFV is $\mu^+ \rightarrow e^+\gamma$ [1]. In SUSY and SUSY-GUT theories, predictions for this process have branching ratio ranging from 10^{-14} to 10^{-12}. This range overlaps significantly with the sensitivity of the MEG experiment at the Paul Scherrer Institut (PSI) in Switzerland. The experiment has taken data in the period 2009-2013 and has recently published the upper limit of $<4.2\times10^{-13}$ at 90 %CL [2]. In order to improve this result, the experiment is currently in an upgrade phase [3] (see Figure 1 and in Table 1 the comparison of the performances of the MEG I and MEG II experiment). The main improvement is the tracker replacement in order to increase the spectrometer granularity and resolution. The MEG Lecce group is involved both for the new drift chamber construction and for the relative front-end electronics development.

2. The positron tracker

The positron tracker is a high transparency, single volume, full stereo, cylindrical Drift Chamber (CDCH) [4], immersed in a non uniform longitudinal B-field, co-axial to the muon beam line with a length of 1.93 m, inner radius of 17 cm, to sweep low energy positrons out of the sensitive volume, and outer radius of 30 cm, to fully contain 52.8 MeV/c positrons. It is composed of 10 concentric layers (Figure 2), divided in 12 identical 30° sectors per layer, 16 drift cells wide. Each layer consists of a sense wires plane between two field wires planes at alternating signs stereo angles (approximately 8°) with respect to contiguous layers for a precise reconstruction of the lon-

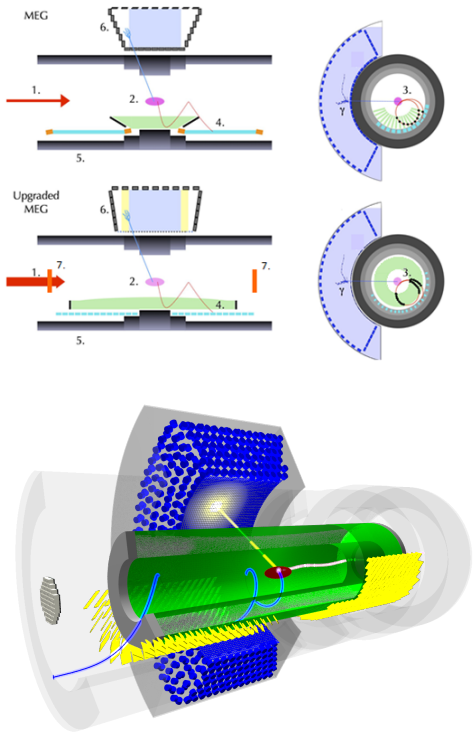

Figure 1. Above: Overview of the MEG upgrade compared with the present MEG configuration: (1) muon beam (7×10^7 μ/s), (2) muon stopping target (140 μm), (3) drift chamber system, (4) timing counters, (5) TDAQ, (6) LXe detector and (7) RMD detectors. Below: Below: Schematic view of the MEG II spectrometer

Table 1
Comparison between MEG design and obtained resolutions with the upgrade detector performance. In bold the resolutions specific of the drift chamber are indicated

Variable	MEG	MEG Upgr
$\triangle E_\gamma$ (%)	1.7	1.0
$\triangle t_\gamma$ (ps)	67	$\leq$67
$\triangle\gamma$ position (mm)	4-6	$\sim$2
$\triangle P_e$ **(keV)**	306	$\leq$130
$\triangle\varphi_{e^+}$**(mrad)**	8.7	$\leq$4
$\triangle\theta_{e^+}$**(mrad)**	9.4	$\leq$5
DC eff. (%)	40	88
$\triangle t_{e^+}$ (ps)	107	30
$\triangle t_{e\gamma}$ (ps)	122	80

gitudinal coordinate. The double readout of the wires with the techniques of charge division and of time propagation difference, together with the ability to implement the cluster counting-timing technique, will further improve the longitudinal coordinate measurement. The stereo configuration of wires gives a hyperbolic profile to the active volume along the z axis. The single drift cell (Figure 2) is approximately square, 6 mm (in the innermost layer) to 8 mm (in the outermost one) wide, with a 20 μm gold plated Tungsten sense wire surrounded by 40 μm silver plated Aluminum field wires in a ratio of 5:1. For equalizing the gain of the innermost and outermost layers, two guard wires layers (50 μm silver-plated Aluminum) have been added at proper radii and at appropriate voltages. The total number of wires amounts to 13056 for an equivalent radiation length per track turn of about 1.45x10^{-3} X_0 when the chamber is filled with an ultra-low mass, gas mixture of helium and iso-butane in the ratio 85:15. Several prototypes have been realized and tested in order to guarantee an efficient operation performance. In particular single hit resolution and the aging have been tested. Single-hit resolution measured on three different prototypes [5] amount to about 110 μm. However in the final chamber further improvements are expected with the new front-end electronics with a 1 GHz bandwidth allowing for the exploitation of the cluster-timing technique. The MEG II Chamber must withstand a particle flux more intense than in MEG I. Several prototypes were studied concerning the performances of the chamber as a function of the collected charge. The high particle flux poses no problem for the DC at least for three years operation with a gain losses of less than 10% per DAQ year of the innermost wires.

Due to the high wire density (12 wires/cm^2), the use of the classical feed-through technique as wire anchoring system could hardly be implemented and therefore it was necessary to develop new wiring strategies. The number of wires and the stringent requirements on the precision of their position and on the uniformity of the wire mechanical tension because of electrostatic wire stability impose the use of an automatic system (Wiring Robot), to operate the wiring procedures. In the next sections we describe the technique of construction of the drift chamber.

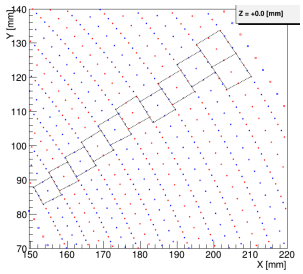

Figure 2. Drift cells configuration at the center of COBRA.

2.1. The wiring robot

The wiring robot (Figure 3) [6,7] has been designed for:

- winding a large number of densely spaced wires;
- applying to the wires the desired mechanical tension and maintaining it constant;
- positioning the wires with high precision;
- fixing the wires on the PCB with a contact-less soldering system.

In order to fulfill all these constraints, the wiring robot, designed and built at the INFN Lecce and University of Salento laboratories, consists of:

- **WIRING SYSTEM:** a semiautomatic wiring machine with a high precision on wire mechanical tensioning (<0.1 g) and on wire positioning (<20 μm) for simultaneous wiring of multi-wire layers;
- **SOLDERING SYSTEM:** a contact-less infrared laser soldering tool [9];
- **EXTRACTION SYSTEM:** an automatic handling system for storing and transporting the multi-wires layers.

All subsystems of the wiring robot are managed and synchronized with a real-time system, based on a National Instrument CompactRIO platform [8] and controlled by a custom made software [9].

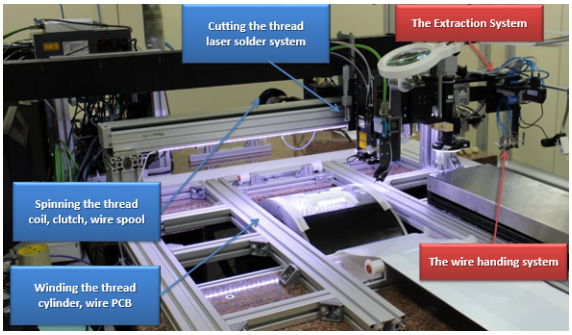

Figure 3. The Wiring Robot.

3. Front–end electronics board

The characteristics of the drift chamber signal establish Front End Electronics requirements. The time separation between different ionizations clusters goes from a few nanoseconds to a few tens of nanoseconds. The read–out interface, therefore, has to be able to process signals with bandwidths of the order of 1 GHz. In order to separate in time the single pulses due to the different ionization clusters, a large signal sampling rate and a low noise and distortion electronics is necessary. Front End electronics is a multichannel board based on a double stage gain amplifier performed using commercial devices such as ADA4927 by Analog Device [11] and THS4509 by Texas Instruments [12], providing a gainbandwidth product of the order of 10 GHz. In order to balance the attenuation of the output cable, a pre-emphasis on both gain stages has been implemented. The FE board is depicted in Figure 4 and the single channel schematic is represented in Figure 5.

4. Conclusion

The DC is one of the major improvements of the MEG upgrade. The expected improvements on the positrons momentum and on the angular resolutions are approximately of a factor three and of a factor two respectively. The drift chamber acceptance improves by a factor two. The performance of the new positron spectrometer

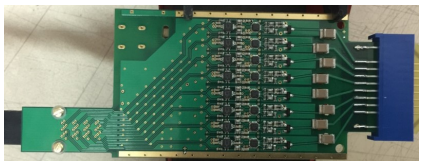

Figure 4. The Front End board.

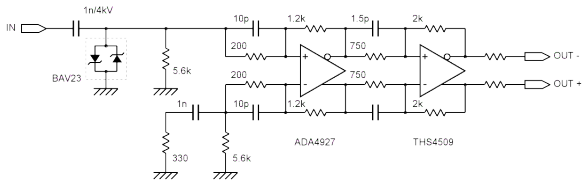

Figure 5. Single channel schematic of the FE.

will contribute to improve MEG results by one order of magnitude. The DC will start commissioning at PSI at the end of summer 2017.

REFERENCES

1. L. Calibbi *et al.*, Eur. Phys. J. C (2014) pg.74-3211, arxiv:1408.0754[hep-phy].
2. A.M. Baldini *et al.*, Eur. Phys. J. C (2016) pg.76:434, arxiv:1605.05081[hep-phy].
3. A. Baldini *et al.*. (MEG Collaboration), arxiv:1301.7225[physics.ins–det].
4. A.M. Baldini *et al.*, Nucl. Instr. and Meth. A **824** (2016) pg.589-591, DOI:10.1016/j.nima.2015.10.103.
5. A.M. Baldini *et al.*, JInstr **11** (2016), arXiv:1605.07970.
6. G. Chiarello *et al.*, Nucl. Instr. and Meth. A **824** (2016) pg.512-514, DOI:10.1016/j.nima.2015.12.021
7. G. Chiarello *et al.*, IWASI (2016), DOI:10.1109/IWASI.2015.7184938.
8. National Instrument, http://www.ni.com/compactrio/.
9. National Instrument, http://www.ni.com/labview.
10. Dr. Mergenthaler GmbH & Co. KG, http://www.ma-info.de/en/lascon-hybrid.html.
11. Anolog Device ADA4927, http://www.analog.com/media/en/technical-documentation/data-sheets/ADA4927-1_ADA4927-2.pdf
12. Texas Instruments THS4509, http://www.ti.com/lit/ds/slos454h/slos454h.pdf